Journal of Peptide Science
J. Peptide Sci. **10**: 160–172 (2004)
Published online 23 September 2003 in Wiley InterScience (www.interscience.wiley.com). DOI: 10.1002/psc.507

JOURNAL OF PEPTIDE SCIENCE

Peptide Helices with Pendant Cycloalkane Rings. Characterization of Conformations of 1-Aminocyclooctane-1-Carboxylic Acid (Ac_8c) Residues in Peptides

SAUMEN DATTA,[a] R. N. S. RATHORE,[a] S. VIJAYALAKSHMI,[c] PREMA G. VASUDEV,[a] R. BALAJI RAO,[c] P. BALARAM[b] and N. SHAMALA[a]*

[a] Department of Physics, Indian Institute of Science, Bangalore-560012, India
[b] Molecular Biophysics Unit, Indian Institute of Science, Bangalore-560012, India
[c] Department of Chemistry, Banaras Hindu University, Varanasi-221005, India

Received 28 February 2003
Accepted 13 May 2003

Abstract: A pentapeptide, Boc-Leu-Ac_8c-Ala-Leu-Ac_8c-OMe **1**, an octapeptide, Boc-Leu-Ac_8c-Ala-Leu-Ac_8c-Ala-Leu-Ac_8c-OMe **2** and a tripeptide, Boc-Aib-Ac_8c-Aib-OMe **3** containing the 1-aminocyclooctane-1-carboxylic acid residue (Ac_8c) were synthesized and conformationally characterized by x-ray diffraction studies in the crystal state. Peptides **1** and **2** were also studied by NMR in $CDCl_3$ solution. Peptide **1** adopts a purely 3_{10}-helical conformation in crystals, stabilized by three intramolecular $1 \leftarrow 4$ hydrogen bonds. Peptide **2** in crystals is largely 3_{10}-helical with distortion in the backbone at the *N*-terminus by the insertion of a water molecule between Ac_8c (2) CO and Ala (6) NH groups. Peptide **3** forms a C_{10}-ring structure, i.e. a type III (III′) β- turn conformation stabilized by an intramolecular $1 \leftarrow 4$ hydrogen bond. Five cyclooctane rings assume boat–chair conformations, whereas the sixth [Ac_8c(8) in **2**] is appreciably distorted, resembling a chiral intermediate in the pseudorotational pathway from the boat–chair to the twisted boat–chair conformation. Internal bond angles of the cyclooctane rings are appreciably distorted from the tetrahedral value, a characteristic feature of the cyclooctane ring. Peptide **1** crystallized in the space group $P2_12_12_1$ with $a = 11.900(4)$ Å, $b = 18.728(6)$ Å, $c = 20.471(3)$ Å and $Z = 4$. The final R_1 and wR_2 values are 0.0753 and 0.2107, respectively, for 3901 observed reflections [$F_o \geq 3\sigma(F_o)$]. Peptide **2** crystallized in space group $P2_1$ with $a = 12.961(5)$ Å, $b = 17.710(10)$ Å, $c = 15.101(7)$ Å, $\beta = 108.45(4)^\circ$ and $Z = 2$. The final R_1 and wR_2 values are 0.0906 and 0.1832, respectively, for 2743 observed reflections [$F_o \geq 3\sigma(F_o)$]. ^{1}H-NMR studies on both the peptides strongly suggest the persistence of 3_{10}-helical conformations in solution. Peptide **3** crystallized in the space group $P2_1/n$, with $a = 10.018(1)$ Å, $b = 20.725(1)$ Å, $c = 12.915(1)$ Å and $Z = 4$. The final R_1 and wR_2 values are 0.0411 and 0.1105, respectively, for 3634 observed reflections [$F_o \geq 4\sigma(F_o)$]. Copyright © 2003 European Peptide Society and John Wiley & Sons, Ltd.

Keywords: 1-aminocyclooctane-1-carboxylic acid; cycloalkanes; peptide conformation; peptide helices

INTRODUCTION

Backbone modifications are being widely investigated as a means of controlling chain stereochemistry in the design of analogues of biologically active peptides [1–3] and in the construction of synthetic mimics of protein structures [4–6]. $C^{\alpha,\alpha}$-Dialkylated amino acid residues, containing both linear and cycloalkane side-chains, have been shown to strongly stabilize helical conformations [7–12]. The use of 1-aminocycloalkane-1-carboxylic acid residues permits the introduction of completely hydrophobic side-chains with limited

* Correspondence to: Dr N. Shamala, Department of Physics, Indian Institute of Science, Bangalore-560012, India;
e-mail: shamala@physics.iisc.ernet.in
Contract/grant sponsor: Department of Science and Technology, Government of India; Contract/grant number: SP/SO/D-08/95.

conformational flexibility. Thus far, only relatively short peptides containing 1-aminocycloalkane-1-carboxylic acids (Ac_nc) have been structurally characterized for ring sizes (n) ranging from 3 to 12 membered rings [8,13–18]. The crystallinity of apolar peptide helices provides an entry to the crystallographic characterization of large, flexible cycloalkane rings. A systematic comparison of the conformational properties of $C^{\alpha,\alpha}$-dialkylated amino acids with acyclic and cyclic side-chains has been performed. This paper reports a structural analysis of three, five and eight residue peptides containing 1-aminocyclooctane-1-carboxylic acid (Ac_8c). The sequences, Boc-Leu-Ac_8c-Ala-Leu-Ac_8c-OMe (peptide **1**) and Boc-Leu-Ac_8c-Ala-Leu-Ac_8c-Ala-Leu-Ac_8c-OMe (peptide **2**), were chosen to place the cyclooctane ring approximately on the same face of the cylindrical $3_{10}/\alpha$-helical structures. Boc-Aib-Ac_8c-Aib-OMe (peptide **3**) is a potential model β-turn forming tripeptide incorporating Ac_8c at the $i+2$ position.

MATERIALS AND METHODS

Peptide Synthesis

The peptides **1**–**3** were synthesized by conventional solution phase procedures using a fragment condensation strategy. The Boc group was used for *N*-terminal protection and the *C*-terminus was protected as a methyl ester. Deprotections were performed using 98% formic acid or saponification, respectively. Couplings were mediated by N,N′-dicyclohexylcarbodiimide/1-hydroxy-1,2,3-benzotriazole (DCC/HOBt). The intermediate peptides were characterized by ^{1}H-NMR (80 MHz) and thin-layer chromatography (TLC) and were used without further purification. The final peptides were purified by medium-pressure liquid chromatography (MPLC) on a reverse-phase C_{18} column. Homogeneity was established by HPLC on a 5μ C_{18} column. The peptides were fully characterized by ^{1}H NMR.

The pentapeptide **1** was synthesized using a $2+3$ strategy involving coupling of Boc-Leu-Ac_8c-OH to H-Ala-Leu-Ac_8c-OMe, which in turn was obtained by formic acid deprotection of Boc-Ala-Leu-Ac_8c-OMe. Peptide **1** was obtained as a white solid which was completely characterized by 500 MHz ^{1}H-NMR spectroscopy. Chemical shifts are listed in Table 7.

FABMS: $[M+H]^+$ 736; $[M+Na]^+$ 758.

The octapeptide **2** was synthesized by the $2+6$ strategy involving coupling of Boc-Leu-Ac_8c-OH to H-Ala-Leu-Ac_8c-Ala-Leu-Ac_8c-OMe. The latter was synthesized by coupling Boc-Ala-OH to H-Leu-Ac_8c-Ala-Leu-Ac_8c-OMe, generated by 98% formic acid deprotection of peptide **1**. The peptide was fully characterized by 500 MHz ^{1}H NMR. Chemical shifts are listed in Table 7. Homogeneity was demonstrated by analytical HPLC.

The tripeptide Boc-Aib-Ac_8c-Aib-OMe was synthesized by sequential extension from the *N*-terminus. Boc-Aib-OH was coupled to H-Ac_8c-OMe to yield Boc-Aib-Ac_8c-OMe. Saponification yielded Boc-Aib-Ac_8c-OH which was then coupled to H-Aib-OMe to yield the tripeptide as a white solid. M.P. = 180°–182 °C. The peptide was characterized by 80 MHz ^{1}H NMR.

NMR Studies

All NMR experiments were carried out on Bruker AMX-400 and Bruker DRX-500 spectrometers at the Sophisticated Instrument Facility, Indian Institute of Science, Bangalore. Peptide concentrations were in the range 5–6 mM. Resonance assignments were performed using two-dimensional double quantum filtered COSY and rotating frame nuclear Overhauser effect (ROESY) experiments. All 2D data were acquired at 1K data points, 512 experiments with 48–64 transients. A 300 ms mixing time was used for ROESY experiments. The spectral width for all the experiments was set to 4500 Hz. NMR data were processed using the UXNMR or the FELIX software. All two-dimensional data sets were zero filled to 1024 points with a 90° phase shifted squared sine-bell filter in both dimensions. The probe temperature was maintained at 303 K.

Crystallization and X-Ray Diffraction

Crystals of peptide **1**–**3** were grown by slow evaporation from methanol/water mixtures (for peptides **1** and **2**) and acetonitrile (for peptide **3**), respectively. X-ray diffraction data were collected from dry crystals on an automated four-circle diffractometer. Unit cell parameters were obtained and refined by a least squares fit of the angular settings of 25 accurately determined small angle reflections. Three-dimensional CuK_α intensity data were collected to $2\theta = 150°$ for peptide **1** and $2\theta = 140°$ for peptide **3.** MoK_α intensity data was collected to $2\theta = 50°$ for peptide **2**. ω-2θ scans with variable speeds were used. Two reflections were

monitored after every 100 reflections (the intensity remained constant within 3%). Lorentz polarization corrections were applied, but not the absorption corrections [μ (peptide **1**) = 0.60 mm^{-1}, μ (peptide **2**) = 0.08 mm^{-1}, μ (peptide **3**) = 0.66 mm^{-1}].

Crystal Structure Determination and Refinement

The structures were solved by direct phase determination methods using the random-tangent formula procedure in the SHELXS-86 [19] (peptides **1** and **2**) and SHELXS-97 [20] (peptide **3**) computer programs. A full matrix least-squares refinement was carried out using SHELXL-93 [21] (peptides **1** and **2**) and SHELXL-97 [22] (peptide **3**). All the non-hydrogen atoms were initially refined isotropically and then anisotropically. The hydrogen atoms were fixed geometrically in the idealized positions with C–H = 1.08 Å and N–H = 1.08 Å and refined in the final cycle as riding over the atoms to which they are bonded. In the refinement for peptides **1** and **2** restraints were applied on bond lengths and bond angles in three of the six cyclooctane rings [C3-C_4, C_4-C_5, C_5-C_6, C_6-C_7, $\angle C_3C_4C_5$, $\angle C_4C_5C_6$ and $\angle C_6C_7C_8$ in Ac_8c(2) of peptide **1**; C_3-C_4, C_4-C_5, C_5-C_6, C_6-C_7, $\angle C_4C_5C_6$ and $\angle C_5C_6C_7$ in Ac_8c(5) and C_2-C_3, C_3-C_4, C_4-C_5, C_5-C_6, C_6-C_7, $\angle C_3C_4C_5$, $\angle C_4C_5C_6$ and $\angle C_5C_6C_7$ in Ac_8c(8) of peptide **2**].The final R-factors for peptides **1**–**3** were 0.0753 (R_w = 0.2107), 0.0906 (R_w = 0.1832), and 0.0411 (R_w = 0.1105) for 3901, 2743 and 3634 observed reflections, respectively, with $F_o \geq 3\sigma(F_o)$ for peptides **1** and **2** and $F_o \geq 4\sigma(F_o)$ for peptide **3**. The function minimized during refinement for peptides **1** and **3** was $\sum w(|F_o - F|)^2$ where $w = 1/[\sigma^2 \times (F_o^2) + (0.1587 \times P)^2 + 0.44P]$ for peptide **1** and $w = 1/[\sigma^2 \times (F_o^2) + (0.0581 \times P)^2 + 0.45P]$ for peptide **3** where $P = (\max(F_o^2, 0) + 2 \times F_c^2)/3$. The function minimized during refinement for peptide **2** was $\sum w(|F_o - F|)^2$ where $w = 1/[\sigma^2 \times (F_o^2) + (0.1 \times P)^2]$.

Table 1 Crystal Data and Structure Refinement Details for Peptides **1**–**3**

	Peptide **1**	Peptide **2**	Peptide **3**
Empirical formula	$C_{39}O_8N_5H_{69}$	$C_{57}O_{11}N_8H_{100}$	$C_{23}H_{41}N_3O_6$
Crystal size (mm)	0.04 × 0.50 × 1.20	0.20 × 0.30 × 0.80	1.02 × 0.26 × 0.20
Crystallization solvent	CH_3OH/H_2O	CH_3OH/H_2O	CH_3CN
Space group	$P\,2_12_12_1$	$P2_1$	$P2_1/n$
Cell parameters			
a (Å)	11.900 (4)	12.961 (5)	10.018 (1)
b (Å)	18.728 (6)	17.710 (10)	20.725 (1)
c (Å)	20.471 (3)	15.101 (7)	12.915 (1)
α (deg)	90	90	90
β (deg)	90	108.45 (4)	91.18 (1)
γ (deg)	90	90	90
Volume (Å^3)	4562.4	3288.1	2680.9
Z	4	2	4
Co-crystallized solvent	None	Water	None
Molecular weight	736.00	1089.45	455.49
Density (g/cm^3)	1.072	1.100	1.129
F(000)	1608	1188	992
Radiation (Å)	CuK_α (λ = 1.5418)	MoK_α (λ = 0.7107)	CuK_α (λ = 1.5418)
2θ Max (°)	150	50	140
Scan type	ω-2θ	ω-2θ	ω-2θ
Independent reflections	5191	5980	4868
Observed reflections	3901 [$\|F\| > 3\sigma(F)$]	2743 [$\|F\| > 3\sigma(F)$]	3634 [$\|F\| > 4\sigma(F)$]
Goodness-of-fit (S)	1.110	1.002	1.041
$\Delta\rho_{max}$ (eÅ^{-3})	0.30	0.24	0.21
$\Delta\rho_{min}$ (eÅ^{-3})	−0.37	−0.50	−0.14
Final R index	0.0753	0.0906	0.0411
Final R_w index	0.2107	0.1832	0.1105
Data/restraints/parameters	3901/7/536	2743/14/793	3634/0/290

All the crystallographic parameters related to the data collection and refinement are given in Table 1. Crystallographic data (excluding structure factors) for peptides **1**, **2** and **3** have been deposited with the Cambridge Crystallographic Data Centre as supplementary publication numbers CCDC-208280, CCDC-208279 and CCDC-208278, respectively. Copies of the data can be obtained, free of charge, on application to CCDC, 12 Union Road, Cambridge CB2 1EZ, UK, (fax: +44 1223 336033 or E-mail: deposit@ccdc.cam.ac.uk)

RESULTS AND DISCUSSION

Structure of Peptides in Crystals

Peptide 1. Figure 1 shows a stereoview of the structure of pentapeptide **1**. From the backbone torsion angles summarized in Table 2, it is evident that residues 1–4 adopt ϕ, ψ values in the $3_{10}/\alpha$-helical region of the conformational space. Table 3 lists relevant parameters for *potential* hydrogen bond interactions. The molecule clearly possesses three intramolecular $1 \leftarrow 4$ hydrogen bonds, resulting in the formation of a short stretch of 3_{10}-helix.

Peptide 2. A stereoview of the molecular conformation of octapeptide **2** is shown in Figure 2. From the backbone torsion angles given in Table 2 it is clear that residues 1–7 cluster in the right-handed helical region of the ϕ, ψ space. Inspection of *potential* hydrogen bond parameters listed in Table 4 reveals that four potential $1 \leftarrow 4$ hydrogen bonds can be identified, characterizing the largely 3_{10}-helix structure. The Leu (1) CO group shows evidence for formation of a 'three-centre hydrogen bond', involving donor NH groups of Leu (4) and Ac_8c (5) residues. Such 'three-centre hydrogen bond' is relatively common at helix termini in peptide structures [23–26]. A lone water molecule inserts into the helix backbone forming hydrogen bonds to Ala (6) NH and Ac_8c (2) CO groups. The inserted water is positioned to interact also with the Ala (3) CO groups (Table 4). Solvent insertion into a helical backbone is also a relatively common occurrence in the crystal structure of peptide helices [25,27–30].

Figure 3 shows a superposition of residues 1–5 of peptide **1** with residues 4–8 of peptide **2**. The close similarity of the backbone fold and side-chain orientation of the pentapeptide segment are

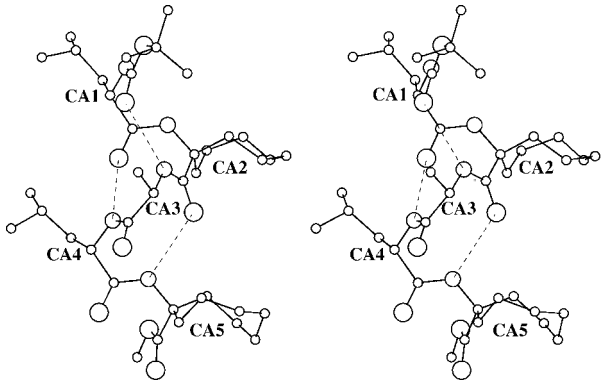

Figure 1 Stereo view of pentapeptide **1** in crystals. Intramolecular hydrogen bonds are indicated by broken lines.

Table 2 Backbone and Side-Chain Torsion Angles* (deg)

Residue	ϕ	ψ	ω	χ^1	χ^2
Peptide 1					
Leu(1)	−62[a]	−28	177	−63	−53/176
Ac_8c(2)	−54	−27	−178		
Ala(3)	−66	−11	172		
Leu(4)	−67	−24	169	−70	−70/164
Ac_8c(5)	46	55[b]	175[c]		
Peptide 2					
Leu(1)	−58[a]	−36	−173	−74	−58/176
Ac_8c(2)	−56	−35	180		
Ala(3)	−75	−41	−171		
Leu(4)	−84	−23	−170	−60	−63/168
Ac_8c(5)	−51	−45	−172		
Ala(6)	−65	−21	180		
Leu(7)	−83	−21	−171	−58	−56/179
Ac_8c(8)	46	48[d]	180[e]		
Peptide 3					
Aib(1)	±59[a]	±35	±174		
Ac_8c(2)	±56	±31	±178		
Aib(3)	±48	±48[f]	±180[g]		

* The torsion angles for rotation about bonds of the peptide backbone (ϕ, ψ, and ω) and about bonds of the amino acid side chains (χ^1, χ^2) are given as suggested by the IUPAC-IUB Commission on Biochemical Nomenclature (1970) [43]. Estimated standard deviations ~1.0° Side-chain torsion angles corresponding to the cyclooctane ring of all the Ac_8c residues are given in Figure 8.
[a] C′(0)-N(1)-C$^\alpha$(1)-C′(1).
[b] N(5)-C$^\alpha$(5)-C′(5)-O(OMe).
[c] C$^\alpha$(5)-C′(5)-O(OMe)-C(OMe).
[d] N(8)-C$^\alpha$(8)-C′(8)-O(OMe).
[e] C$^\alpha$(8)-C′(8)-O(OMe)-C(OMe).
[f] N(3)-C$^\alpha$(3)-C′(3)-O(OMe).
[g] C$^\alpha$(3)-C′(3)-O(OMe)-C(OMe).

Table 3 Potential 1 ← 4 and 1 ← 5 Hydrogen Bonds Parameters in Boc-Leu-Ac_8c-Ala-Leu-Ac_8c-OMe (Peptide **1**)

Type	Donor	Acceptor	N···O (Å)	H···O (Å)	C=O···H (deg)	C=O···N (deg)	O···H–N (deg)
			Intramolecular				
1 ← 4[b]	N(3)	O(0)	2.95	2.13	121	126	159
1 ← 4[b]	N(4)	O(1)	3.03	2.18	128	130	171
1 ← 4[b]	N(5)	O(2)	3.05	2.27	123	128	151
1 ← 5	N(4)	O(0)	4.56	4.00	134	142	126
1 ← 5	N(5)	O(1)	4.76	4.08	131	137	138
			Intermolecular				
	N(1)	O(4)[a]	2.91	2.06	150	150	176
	N(2)	O(5)[a]	3.10	2.40	150	156	139

[a] Symmetrically related by ($x - 1$, y, z).
[b] These are the acceptable hydrogen bonds satisfying the criteria of hydrogen bond geometry [44,45].

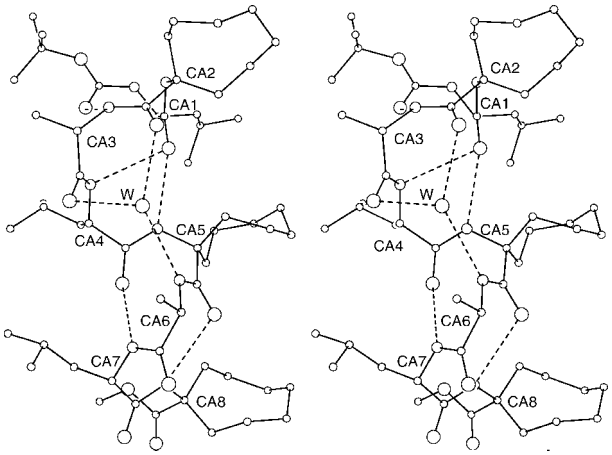

Figure 2 Stereo view of octapeptide **2** in crystals. Intramolecular hydrogen bonds are indicated by broken lines.

evident. In both peptides the achiral Ac_8c residue at the *C*-terminus adopts ϕ, ψ values that lie in the left-handed helical region. Chiral reversal of conformational angles at the *C*-terminus has been frequently observed in peptide ester helices containing Aib residues [31–33]. The reason for this inversion of handedness is probably due to the crystal packing forces and the need of formation of appropriate intermolecular hydrogen bonds.

Peptide 3. Figure 4 shows a stereoview of the structure of tripeptide **3**. From the backbone torsion angles given in Table 2 it is clear that all the three residues lie in the (right or left) helical region of the conformational map. Both senses

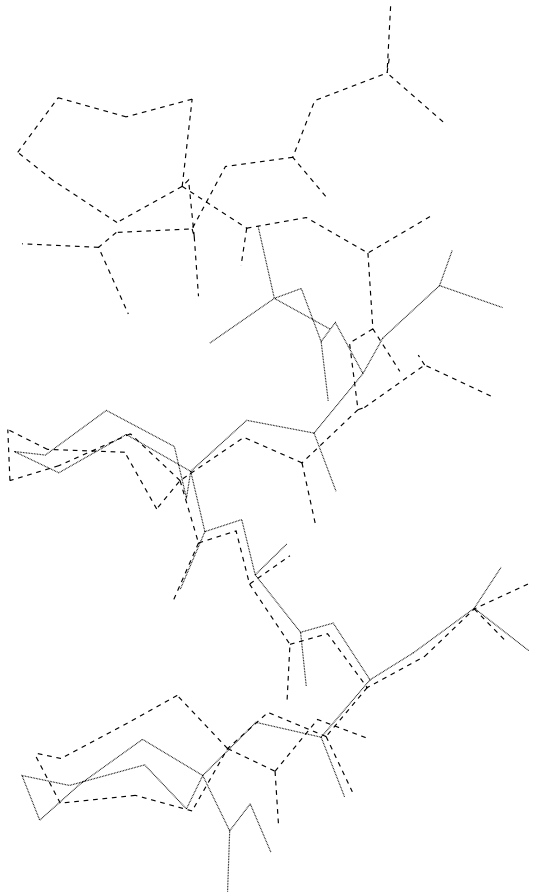

Figure 3 Superposition of the structure of the pentapeptide **1** (Boc-Leu-Ac_8c-Ala-Leu-Ac_8c-OMe) and the octapeptide **2** (Boc-Leu-Ac_8c-Ala-Leu-Ac_8c-Ala-Leu-Ac_8c-OMe). The former is indicated by the solid line, while the latter is represented by the broken line.

Table 4 Potential 1 ← 4 and 1 ← 5 Hydrogen Bonds Parameters in Boc-Leu-Ac_8c-Ala-Leu-Ac_8c-Ala-Leu-Ac_8c-OMe (Peptide **2**)

Type	Donor	Acceptor	N···O (Å)	H···O (Å)	C=O···H (deg)	C=O···N (deg)	O···H–N (deg)
				Intramolecular			
1 ← 4[b]	N(3)	O(0)	3.12	2.44	114	123	136
1 ← 4[b]	N(4)	O(1)	3.10	2.54	100	112	123
1 ← 4	N(5)	O(2)	4.22	3.48	82	89	145
1 ← 4	N(6)	O(3)	4.47	3.71	100	102	148
1 ← 4[b]	N(7)	O(4)	2.95	2.15	124	131	153
1 ← 4[b]	N(8)	O(5)	3.17	2.37	112	118	156
1 ← 5	N(4)	O(0)	3.39	2.60	146	153	152
1 ← 5[b]	N(5)	O(1)	2.95	2.23	161	164	142
1 ← 5	N(6)	O(2)	5.16	4.38	122	122	152
1 ← 5	N(7)	O(3)	5.29	4.57	116	122	143
1 ← 5	N(8)	O(4)	3.76	3.17	143	152	128
				Intermolecular			
	N(1)	O(8)[a]	3.19	2.38	112	113	157
	N(2)	O(7)[a]	3.01	2.16	141	139	171
			N···W/W···O	H···W	C=O···W		W···H–N
	N(6)	W	2.99	2.18			157
	W	O(3)	2.77		97		
	W	O(2)	2.85		136		

[a] Symmetrically related by (x, y, $z-1$).
[b] These are the acceptable hydrogen bonds satisfying the criteria of hydrogen bond geometry [44,45].

of twist are observed because of the absence of chiral residues in the tripeptide, which yields centrosymmetric crystals. Again, the Aib residue at the *C*-terminus of the peptide has ϕ, ψ values with opposite sign to that of preceding residues Aib (1) and Ac_8c (2). Table 5 lists relevant parameters for *potential* hydrogen bond interactions. The molecule clearly possesses one intramolecular 1 ← 4 hydrogen bond, N(3)···O(0), resulting in the formation of a C_{10}-ring structure, i.e. a type III (III′) β-turn conformation.

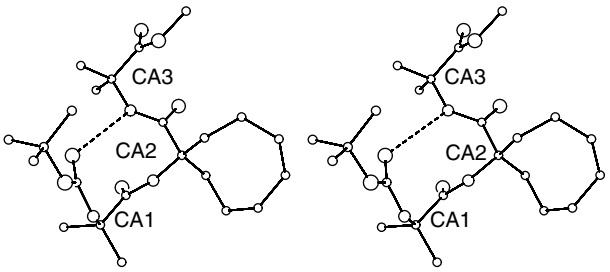

Figure 4 Stereo view of tripeptide **3** in crystals. The intramolecular hydrogen bond is indicated by a broken line.

Molecular Packing

Figure 5 shows a view of the molecular packing in crystal of the octapeptide **2** viewed in a direction perpendicular to the helix axis. Helices are arranged in columns in the normal *head-to-tail* fashion with hydrogen bonds formed between NH groups of one molecule and CO groups of a translationally related molecule, which do not participate in intramolecular hydrogen bonding. In this structure the two intermolecular hydrogen bonds formed between N(1)···O(8) [x, y, z − 1] and N(2)···O(7) [x, y, z − 1] (Table 4) place the helices in perfect register along the crystallographic *c*-axis. Adjacent columns of helices run in antiparallel fashion. An almost identical *head-to-tail* arrangement of the short helix in peptide **1** is formed with intermolecular hydrogen

Table 5 Potential 1 ← 4 Hydrogen Bonds Parameters in Boc-Aib-Ac_8c-Aib-OMe (Peptide **3**)

Type	Donor	Acceptor	N···O (Å)	H···O (Å)	C=O···H (deg)	C=O···N (deg)	O···H–N (deg)
				Intramolecular			
1 ← 4[b]	N(3)	O(0)	3.07	2.27	125	130	155
				Intermolecular			
	N(1)	O(2)[a]	2.98	2.15	164	169	163
	N(2)	O(3)[a]	3.28	2.53	142	148	145

[a] Symmetrically related by $(x + 1/2, -y + 1/2, z + 1/2)$.
[b] These are the acceptable hydrogen bonds satisfying the criteria of hydrogen bond geometry [44,45].

bonds N(1)···O(4) [x − 1, y, z] and N(2)···O(5) [x − 1, y, z] (Table 3) (Figure not shown).

A view of the packing mode in both crystals seen down the helix axis is shown in Figure 6. In pentapeptide **1** molecules are arranged in helical columns which run antiparallel to adjacent columns. Each helix makes close contacts with four antiparallel neighbours. This kind of checkerboard arrangements has been identified earlier by Karle in an analysis of modes of assembly in helical peptide crystals [34].

The assembly of helices in monoclinic crystals of the octapeptide **2** is distinctly different. Helical columns align themselves in parallel fashion to form sheets, consisting of helical arrays which run in antiparallel fashion. The crystal is then formed by alternating layers of helical sheets which run in opposite directions. Each peptide helix in the square grid arrangement makes close contact with two parallel neighbours along the crystallographic *a*-axis and two antiparallel neighbours along the *b*-axis. All interactions between the helices in the direction perpendicular to the helix-axis are of the van der Waals type.

Figure 7 shows a view of the molecular packing in crystal of the tripeptide **3**. In the crystal the molecules of peptide **3** are held together by the formation of two intermolecular N–H···O hydrogen bonds between molecules related by n-glide symmetry: They are N (2)···O (3) [x + 1/2, −y + 1/2, z + 1/2] and N (1)···O (2) [x + 1/2, −y + 1/2, z + 1/2] (Table 5). Molecules related by 2_1 screw symmetry are held together by van der Waals interactions only.

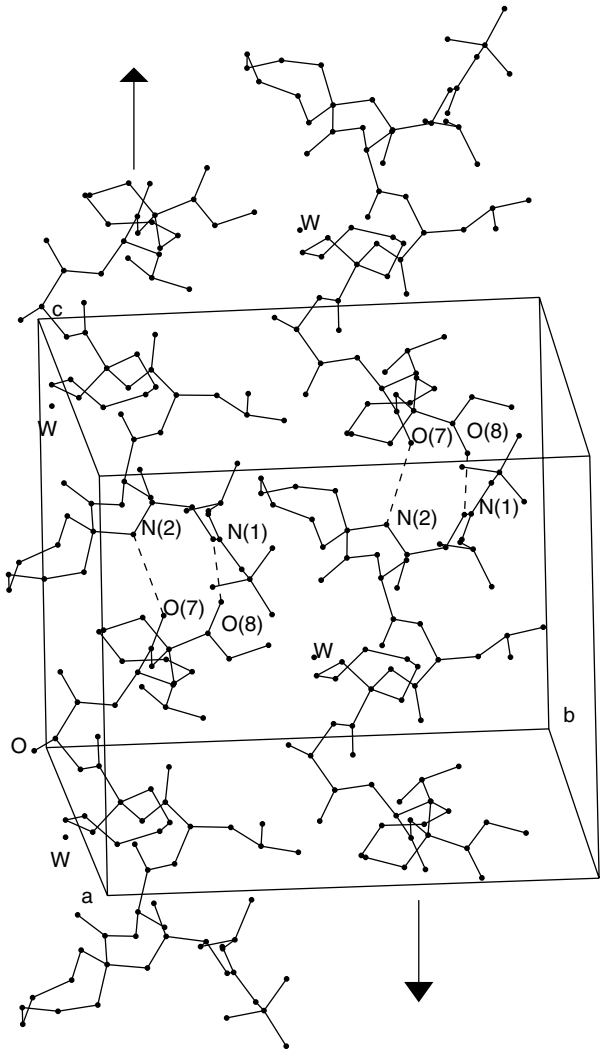

Figure 5 Packing diagram for the octapeptide **2**. View perpendicular to the helix axis. Intermolecular hydrogen bonds are indicated by broken lines. W indicates the oxygen atom of the co-crystallized water molecule.

Cyclooctane Conformations

Figure 8 compares the crystallographically determined conformations of the six cyclooctane rings present in peptides **1**–**3**. Ac_8c(2) [in peptides **1**–**3**]

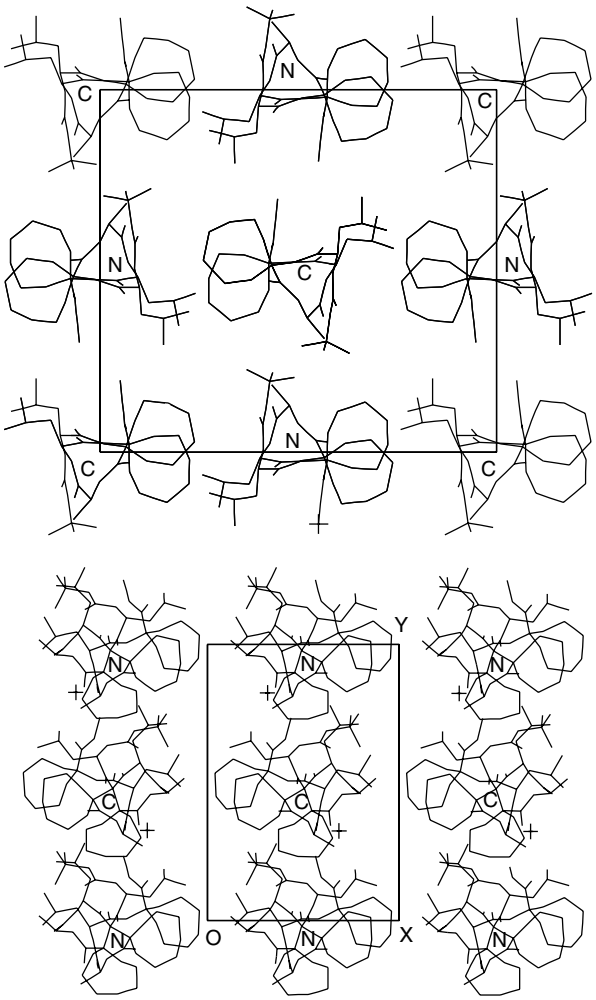

Figure 6 Packing diagrams for peptide **1** (top) and peptide **2** (bottom) viewed down the helix axis.

and $Ac_8c(5)$ [in peptides **1** and **2**] side-chains have adopted boat–chair conformations as originally defined by Hendrickson [35]. The $Ac_8c(8)$ residue in peptide **2** is appreciably distorted, with a rather low value of the dihedral angle C_5-C_6-C_7-C_8 ($\omega_2 = -14^\circ$). This conformation resembles the chiral intermediate in the pseudorotational pathway from the boat–chair to the twisted boat-chair conformations [36]. In all six Ac_8c residues the C^α atom occupies the basal position in the boat segment of the boat–chair conformation. In four cases the amino group occupies the *quasi*-equatorial position, while the carboxylic group is *quasi*-axial, whereas in peptides **1** and **3** the amino group is *quasi*-axial in the $Ac_8c(2)$ residue.

The determination of the geometry of as many as six cyclooctane rings in the structures of peptides

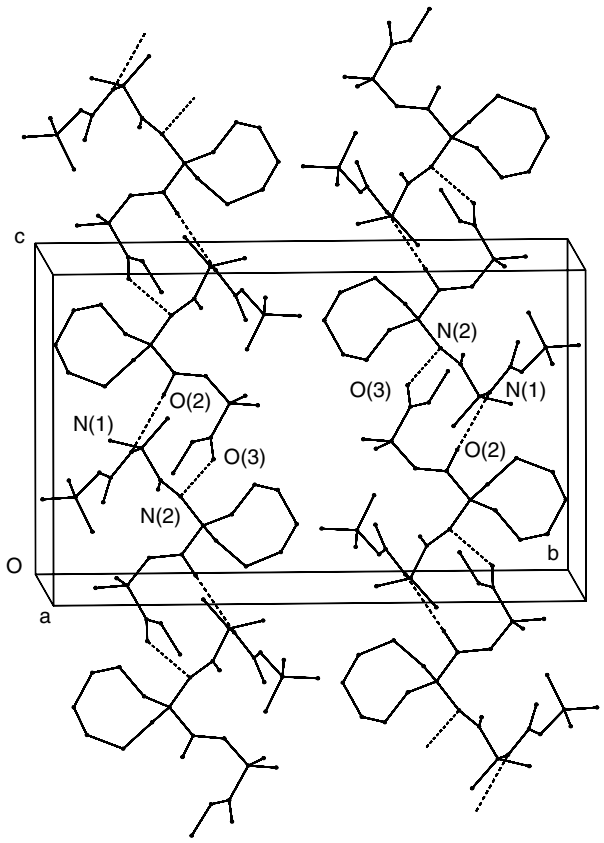

Figure 7 Packing diagram for tripeptide **3**. Intermolecular hydrogen bonds are indicated by broken lines.

1–**3** provides an opportunity to compare the structural characteristics of medium-sized cyclooctane rings. Table 6 lists the internal bond angles in all the six Ac_8c side-chains and provides a comparison with values determined in previous crystal structures, electron diffraction studies of the parent hydrocarbon and in molecular mechanics studies of cyclooctane. The observed internal bond angles in all cases are appreciably larger than the ideal tetrahedral value. The average values [$Ac_8c(2)$: 117.3°], [$Ac_8c(5)$: 116.3°] in peptide **1**, [$Ac_8c(2)$: 117.2°], [$Ac_8c(5)$ 116.2°], [$Ac_8c(8)$: 117.4°] in peptide **2** and [$Ac_8c(2)$: 116.5°] in peptide **3**, obtained from the six cyclooctane rings in the present crystal structure study, are in good agreement with the results of electron diffraction studies (Table 6). In the crystallographic refinement Figure 9 summarizes the distribution of the equivalent temperature factors ($Ueq = (1/3)\sum_i \sum_j U_{ij} a_i^* a_j^* a_i a_j$) for the eight carbon atoms of the Ac_8c rings. Carbon atoms C_4, C_5 and C_6 show the greatest positional variation, a feature not unexpected in the eight-membered ring.

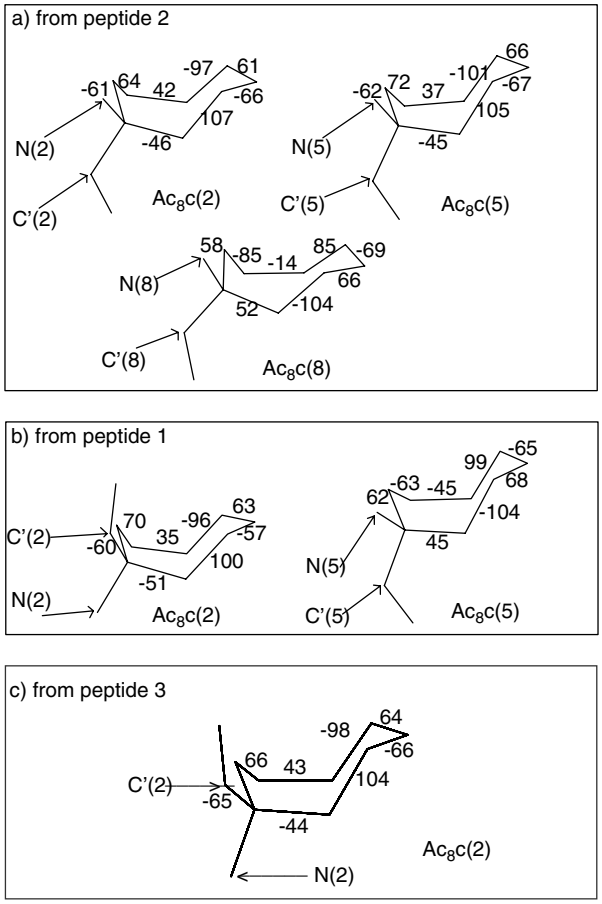

Figure 8 Conformations of the Ac_8c residues of peptides **1**–**3** in crystals. Ring torsion angles are indicated.

Although molecular mechanics calculations have frequently focused on cyclooctane rings in order to explore the possibility of multiple conformational states [35,37–41], accumulated evidence suggests that even in the gas phase the 'boat–chair is either the exclusive or the strongly predominant form' [42]. The present structure determinations confirm the overwhelming preference of cyclooctane rings for the boat–chair conformations with quasi C_S symmetry. Peptide scaffolds with a high degree of crystallinity may be useful in probing structural variability of large ring cycloalkanes.

Solution Conformations

The conformations of peptides **1** and **2** were probed in chloroform solution by 400 MHz ^{1}H-NMR. Resonance assignments were achieved in a straightforward manner using a combination of correlated spectroscopy (COSY) and rotating frame nuclear Overhauser enhancement spectroscopy (ROESY).

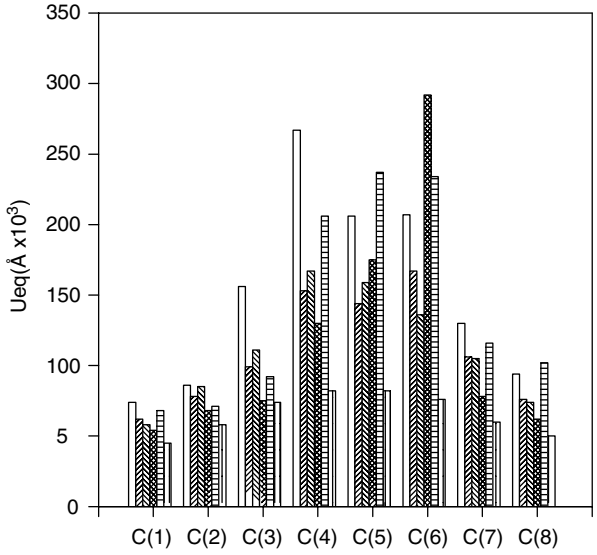

Figure 9 Distribution of equivalent temperature factors of the eight ring carbon atoms in Ac_8c residues of peptides **1**–**3** [bars 1 and 2 from left correspond to $Ac_8c(2)$ and $Ac_8c(5)$ of peptide **1**, bars 3–5 correspond to $Ac_8c(2)$, $Ac_8c(5)$ and $Ac_8c(8)$ of peptide **2**, and bar 6 corresponds to $Ac_8c(2)$ of peptide **3**, respectively].

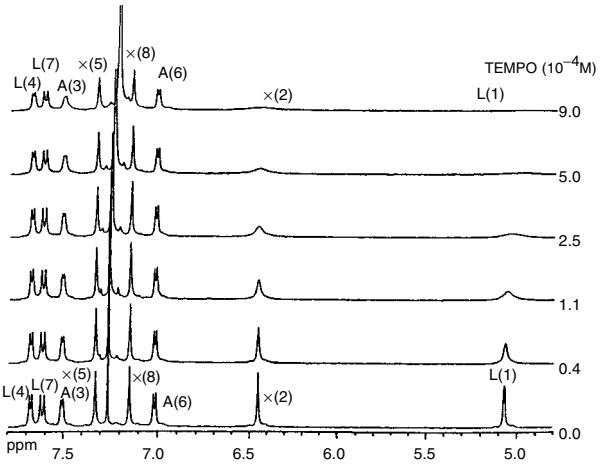

Figure 10 NH proton resonances of octapeptide **2** (400 MHz) in the presence of varying concentrations of the free radical TEMPO. Peptide concentration: 5 mM in $CDCl_3$. TEMPO concentrations are indicated. X = Ac_8c.

Chemical shifts of backbone and side- chain protons are summarized in Table 7. The involvement of peptide NH groups in intramolecular hydrogen bonding was established by solvent perturbation of NH chemical shifts in $CDCl_3/(CD_3)_2SO$ mixtures and by paramagnetic radical-induced line broadening in $CDCl_3$. Figure 10 shows the effect of addition of

Table 6 A Representation of the Calculated and Observed Angles of Cyclooctane in Boat–Chair Conformations

	$C_1-C_2-C_3$	$C_2-C_3-C_4$	$C_3-C_4-C_5$	$C_4-C_5-C_6$	$C_5-C_6-C_7$	$C_6-C_7-C_8$	$C_7-C_8-C_1$	$C_8-C_1-C_2$	Average
Observed									
Peptide **1** (this study)									
$Ac_8c(2)$	115.5	117.2	118.8	120.4	113.3	121.4	117.7	114	117.3
$Ac_8c(5)$	115.4	114.5	119.5	114.5	115.6	119.1	116.6	115.5	116.3
Peptide **2** (this study)									
$Ac_8c(2)$	114.4	119.2	115.4	118.3	119.9	115.6	118.6	116.1	117.2
$Ac_8c(5)$	113.4	120.5	112.7	116.8	117.7	117.2	115.7	115.3	116.2
$Ac_8c(8)$	116.6	117.7	117.7	118.9	120	120.9	114.5	112.7	117.4
Peptide **3** (this study)									
$Ac_8c(2)$	116.7	118.4	116.1	116.8	118.7	114.8	116	114.5	116.5
Moretto *et al.* [17][a]	116.4	117.4	119.9	117.8	118.9	118.4	117.5	114.1	117.5
Dobler *et al.* [46][a]	115	117.3	118.2	118.3	115.6	115.4	115.1	112.7	115.9
Groth [47][a]	116	115.5	118.7	115.8	114.8	117.4	115.2	118	116.5
Bürgi and Dunitz [48][a]	115	115.5	118.3	115.9	118.1	119.9	117.3	114.2	116.8
Egmond and Romers [49][a]	114.2	116.2	119.1	116.4	115.2	117.5	114.8	117.3	116.3
Dorofeeva *et al.* [42][b]	117	116.1	120.2	116.1	117	116	116.1	116	116.8
Calculated									
Hendrickson [37]	113.5	114.3	115.2	114.3	113.5	114.3	115.2	114.3	114.3
Wiberg [50]	109.6	117.4	125.3	117.4	109.6	114	114.4	114	115.2
Bixon and Lipson [51]	114	114	115	113	115	116	116	116	115
Miller and McPhail [52]	115.3	114.3	116.3	114.3	115.3	116.9	116.3	116.9	115.7
Dorofeeva *et al.* [40]	115.3	115	117.4	115	115.3	117.3	116.3	117.3	116.1

[a] Crystal structure determinations of substituted cyclooctane derivatives.
[b] Values obtained from electron diffraction studies of cyclooctane in the gas phase.

2,2,6,6-tetramethylpiperidin-1-oxyl (TEMPO) on the line widths of the NH resonances of octapeptide **2**. It is clearly seen that only two NH resonances, Leu(1) and $Ac_8c(2)$, show appreciable broadening indicative of their solvent exposure. Similarly in pentapeptide **1** the only solvent exposed resonances were Leu(1) and $Ac_8c(2)$ [data not shown]. The solvent shift values ($\Delta\delta$) shown in Table 7 also reveal that in both peptides the only exposed NH groups correspond to those of residues 1 and 2. These results are consistent with the formation of a 3_{10}-helical structure in both the cases in which the NH groups of residues 3 to 5 in peptide **1** and residues 3 to 8 in peptide **2** are intramolecularly hydrogen bonded. The low $^3J_{NHC^{\alpha}H}$ values obtained for most of the Leu and Ala residues (Table 7), with the exception of those at the *C*-terminus, also favour largely helical conformations. In the case of octapeptide **2** all the interresidue $N_iH \leftrightarrow N_{i+1}H$ NOEs (d_{NN}) characteristic of helical conformation were observed [data not shown]. These results confirm that the helical conformations observed in crystals are also a dominant feature in a solvent of low polarity for both peptides.

CONCLUSION

Our results establish that bulky cyclooctane side chains are comfortably accommodated in peptide

Table 7 NMR Parameters for Peptides **1** and **2**[a]

	Chemical shifts (δ ppm)[b]							$^3J_{HNC}$ $^{\alpha}$H
Residue	NH	C^{α} H	C^{β} H	C^{γ} H	C^{δ} H	Others[c]	$\Delta\delta$ (ppm)[d]	(Hz)
Leu(1)	4.99	3.81	1.62	1.50	0.97		1.62	2.5[e]
	(5.11)	(3.80)	(1.61)	(1.48)	(0.94)		(1.46)	(2.8)
Ac8c(2)	6.41	—	—	—	—	1.3–2.3	1.09	—
	(6.48)					(1.3–2.3)	(0.90)	
Ala(3)	7.50	4.07	1.47	—	—		0.01	4.9
	(7.27)	(4.20)	(1.48)				(0.01)	(4.8)
Leu(4)	7.67	3.93	1.78	1.63	0.88		0.16	5.4
	(7.48)	(4.30)	(1.71)	(1.54)	(0.85)		(0.21)	(8.0)
Ac8c(5)	7.32	—	—	—	—	1.3–2.3	0.21	—
	(6.98)					(1.3–2.3)	(0.08)	
Ala(6)	7.01	4.17	1.50	—	—		0.06	5.2
Leu(7)	7.61	4.27	1.72	1.50	0.86		0.02	7.8
Ac8c(8)	7.14	—	—	—	—	1.3–2.3	0.01	—

[a] Values in parentheses are for peptide **1**.
[b] Chemical shift values for proton resonances in $CDCl_3$.
[c] Methylene resonances of Ac_8c residues.
[d] Chemical shift difference for NH protons in $CDCl_3$ and 23 : 77 DMSO-d6/$CDCl_3$.
[e] Value in 0.99 : 99.01 DMSO-d6/$CDCl_3$, added to sharpen resonances.

helices, thus permitting the construction of highly hydrophobic helical faces with large protruding substituents. Expanding the amino acid repertoire to include bulky cycloalkane substituents should provide valuable information in studies of packing in peptide assemblies and also in the design of analogues of biologically active peptides.

Acknowledgements

This research was supported by the Department of Science and Technology, Government of India (grant no: SP/SO/D-08/95). Ms Prema G. Vasudev thanks CSIR, India, for a fellowship.

REFERENCES

1. Goodman M, Ro S. In *Burger's Medicinal Chemistry and Drug Discovery*, Vol. 1, Wolff ME (ed.). Wiley: New York, 1995; 803–861.
2. Toniolo C. Conformationally restricted peptides through short-range cyclizations. *Int. J. Peptide Protein Res.* 1990; **35**: 287–300.
3. Hruby VJ, Obeidi FA, Kazmierski W. Emerging approaches in the molecular design of receptor-selective peptide ligands: conformational, topological and dynamic considerations. *Biochem. J.* 1990; **268**: 249–262.
4. Balaram P. Non-standard aminoacids in peptide design and protein engineering. *Curr. Opin. Struct. Biol.* 1992; **2**: 845–851.
5. Kaul R, Balaram P. Stereochemical control of peptide folding. *Bioorg. Med. Chem.* 1999; **7**: 105–117.
6. Karle IL, Gurunath R, Prasad S, Kaul R, Rao RB, Balaram P. Peptide design: Structural evaluation of potential non-helical segments attached to helical modules. *J. Am. Chem. Soc.* 1995; **117**: 9632–9637.
7. Karle IL, Balaram P. Structural characteristics of α-helical peptide molecules containing Aib residues. *Biochemistry* 1990; **29**: 6747–6756.
8. Paul PKC, Sukumar M, Bardi R, Piazzesi AM, Valle G, Toniolo C, Balaram P. Stereochemically constrained peptides. Theoretical and experimental studies on the conformations of peptides containing 1-aminocyclohexane carboxylic acid. *J. Am. Chem. Soc.* 1986; **108**: 6363–6370.
9. Toniolo C, Benedetti E. Structures of polypeptides from α-amino acids disubstituted at the α-carbon. *Macromolecules* 1991; **24**: 4004–4009.
10. Karle IL, Gurunath R, Prasad S, Rao RB, Balaram P. Crystal structure of a nonapeptide helix containing α,α-di-n-butylglycine (Dbg), Boc-Gly-Dbg-Ala-Val-Ala-Leu-Aib-Val-Leu-OMe. *Int. J. Peptide Protein Res.* 1996; **47**: 376–382.
11. Datta S, Kaul R, Rao RB, Shamala N, Balaram P. Stereochemistry of linking segments in the design of helix-helix motifs in peptides. Crystallographic

comparison of a glycyl-dipropylglycyl-glycyl segment in a tripeptide and a 14-residue peptide. *J. Chem. Soc. Perkin Trans.* **2**: 1997; 1659–1664.
12. Toniolo C, Crisma M, Formaggio F, Peggion C. Control of peptide conformation by the Thorpe-Ingold effect (C^{α}-tetrasubstitution). *Biopolymers (Peptide Sci.)* 2001; **60**: 396–419.
13. Bardi R, Piazzesi AM, Toniolo C, Sukumar M, Antony Raj P, Balaram P. Conformations of peptides containing 1-aminocyclohexane carboxylic acid. Crystal structures of two model peptides. *Int. J. Peptide Protein Res.* 1985; **25**: 628–639.
14. Valle G, Crisma M, Toniolo C, Sudhanand, Rao RB, Sukumar M, Balaram P. Stereochemistry of peptides containing 1-aminocycloheptane-1-carboxylic acid (Ac_7c). Crystal structure of model peptides. *Int. J. Peptide Protein Res.* 1991; **38**: 511–518.
15. Santini A, Barone V, Bavoso A, Benedetti E, Di Blasio B, Fraternali F, Lelj F, Pavone V, Pedone C, Crisma M, Bonora GM, Toniolo C. Structural versatility of peptides from $C^{\alpha,\alpha}$-dialkyl glycines. A conformational energy calculation and x-ray diffraction study of homopeptides from 1-aminocyclopentane-1-carboxylic acid. *Int. J. Biol. Macromol.* 1988; **10**: 292–299.
16. Benedetti E, Di Blasio B, Pavone V, Pedone C, Santini A, Barone V, Fraternali F, Lelj F, Bavoso A, Crisma M, Toniolo C. Structural versatility of peptides from $C^{\alpha,\alpha}$-dialkyl glycines. A conformational energy calculation and x-ray diffraction study of six 1-aminocyclopropane1-carboxylic acid rich peptides. *Int. J. Biol. Macromol.* 1989; **11**: 353–358.
17. Moretto V, Formaggio F, Crisma M, Bonora GM, Toniolo C, Benedetti E, Santini A, Saviano M, Di Blasio B, Pedone C. Preferred conformations of peptides rich in Ac_8c, a medium-ring alicyclic $C^{\alpha,\alpha}$-disubstituted glycine. *J. Peptide Sci.* 1996; **2**: 14–27.
18. Toniolo C, Crisma M, Formaggio F, Benedetti E, Santini A, Iacovino R, Saviano M, Di Blasio B, Pedone C, Kamphuis J. Preferred conformations of peptides rich in alicyclic $C^{\alpha,\alpha}$-disubstituted glycines. *Biopolymers (Peptide Sci.)* 1996; **40**: 519–522.
19. Sheldrick GM. SHELXS-86. *Program for Crystal Structure Determination*. University of Göttingen: Göttingen, Germany, 1986.
20. Sheldrick GM. SHELXS-97. *Program for Crystal Structure Determination*. University of Göttingen: Göttingen, Germany, 1997.
21. Sheldrick GM. SHELXL-93. *Program for Crystal Structure Refinement*. University of Göttingen: Göttingen, Germany, 1993.
22. Sheldrick GM. SHELXL-97. *Program for Crystal Structure Refinement*. University of Göttingen: Göttingen, Germany, 1997.
23. Datta S, Shamala N, Banerjee A, Balaram P. Hydrogen bonding in peptide helices. Analysis of two independent helices in the crystal structure of the peptide Boc-Val-Ala-Leu-Aib-Val-Ala-Phe-OMe. *J. Peptide Res.* 1997; **49**: 604–611.
24. Karle IL, Flippen-Anderson JL, Sukumar M, Balaram P. Parallel and antiparallel aggregation of α-helices; crystal structure of two apolar decapeptides X-Trp-Ile-Ala-Aib-Ile-Val-Aib-Leu-Aib-Pro-OMe (X = Boc, Ac). *Int. J. Peptide Protein Res.* 1990; **35**: 518–526.
25. Karle IL, Flippen-Anderson JL, Uma K, Balaram P. Apolar peptide models for conformational heterogeneity, hydration and packing of polypeptide helices. Crystal structures of hepta- and octapeptides containing α-aminoisobutyric acid. *Proteins: Struct. Funct. Genet.* 1990; **7**: 62–73.
26. Karle IL, Flippen-Anderson JL, Uma K, Balaram H, Balaram P. Peptide design. Influence of a guest Aib-Pro segment on the stereochemistry of an oligo-Val sequence. Solution conformations and crystal structure of Boc-$(Val)_2$-Aib-Pro-$(Val)_3$-OMe. *Biopolymers* 1990; **29**: 1433–1442.
27. Karle IL, Flippen-Anderson JL, Uma K, Balaram P. Aqueous channels within apolar peptide aggregates. A solvated helix of Boc-Aib-Ala-Leu-Aib-Ala-Leu-Aib-Ala-Leu-Aib-OMe $2H_2O.CH_3OH$. *Proc. Natl Acad. Sci. USA* 1988; **85**: 299–303.
28. Karle IL, Flippen-Anderson JL, Uma K, Balaram P. Unfolding of an α-helix in crystals by solvation. Conformational fragility in a heptapeptide. *Biopolymers* 1993; **33**: 827–837.
29. Toniolo C, Peggion C, Crisma M, Formaggio F, Shui X, Eggleston DS. Structure determination of racemic trichogin A IV using centrosymmetric crystals. *Nature Struct. Biol.* 1994; **1**: 908–914.
30. Karle IL, Banerjee A, Bhattacharjya S, Balaram P. Solid state and solution conformations of a helical peptide with a central Gly-Gly segment. *Biopolymers* 1996; **38**: 515–526.
31. Toniolo C, Bonora GM, Bavoso A, Benedetti E, Di Blasio B, Pavone V, Pedone C. Preferred conformations of peptides containing α,α-disubstituted α-amino acids. *Biopolymers* 1983; **22**: 205–215.
32. Karle IL, Flippen-Anderson JL, Uma K, Balaram P. Effects of end group and aggregation on helix conformation. Crystal structure of Ac-(Aib-Val-Ala-Leu)$_2$-Aib-OMe. *J. Peptide Sci.* 1996; **2**: 106–116.
33. Karle IL, Flippen-Anderson JL, Uma V, Balaram P. Accommodation of a D-Phe residue into a right-handed 3_{10}-helix. Structure of Boc-D-Phe-$(Aib)_4$-Gly-Leu-$(Aib)_2$-OMe, an analogue of the amino terminal segment of antiamoebins and emerimicins. *Biopolymers* 1993; **33**: 401–407.
34. Karle IL. Folding, aggregation and molecular recognition in peptides. *Acta Crystallogr.* 1992; **B48**: 341–356.
35. Hendrickson JB. Molecular geometry. IV. The medium rings. *J. Am. Chem. Soc.* 1964; **86**: 4854–4866.
36. Anet FA. Dynamics of eight membered rings in the cyclooctane class. *Top. Curr. Chem.* 1974; **45**: 169–220.

37. Hendrickson JB. Molecular geometry. V. Evaluation of functions and conformations of medium rings. *J. Am. Chem. Soc.* 1967; **89**: 7036–7043.
38. Hendrickson JB. Molecular geometry. VI. Modes of interconversion in medium rings. *J. Am. Chem. Soc.* 1967; **89**: 7047–7061.
39. Burket U, Allinger NL. In *Molecular Mechanics*. *ACS Monograph* 177, American Chemical Society: Washington, DC, 1982; 79–167.
40. Kolossváry I, Guida WC. Low mode search. An efficient automated computational method for conformational analysis. Application to cyclic and acyclic alkanes and cyclic peptides. *J. Am. Chem. Soc.* 1996; **118**: 5011–5019.
41. Still WC, Galynker I. Chemical consequences of conformations in macrocyclic compounds. *Tetrahedron* 1981; **37**: 3981–3996.
42. Dorofeeva OV, Mastryukov VS, Allinger NL, Almenningen A. The molecular structure and conformation of cyclooctane as determined by electron diffraction and molecular mechanics calculations. *J. Phys. Chem.* 1985; **89**: 252–257.
43. IUPAC-IUB Commission on Biochemical Nomenclature. Abbreviation and symbols for the description of the conformations of polypeptide chains. *Biochemistry* 1970; **9**: 3471–3479.
44. Baker EN, Hubbard RE. Hydrogen bonding in globular proteins. *Progr. Biophys. Mol. Biol.* 1984; **44**: 97–179.
45. Toniolo C. Intramolecularly hydrogen bonded peptide conformations. *CRC Crit. Rev. Biochem.* 1980; **9**: 1–44.
46. Dobler M, Dunitz JD, Mugnoli A. Die strukturen der mittleren ringverbindungen. XI. Cyclooctan-1,2-trans-dicarbonsäure. *Helv. Chim. Acta* 1966; **49**: 2492–2502.
47. Groth P. Crystal structure of 3.6.spiro-dicyclooctylidene-1,2,4,5-tetraoxacyclohexane ('dimeric cyclooctanone peroxide'). *Acta Chem. Scand.* 1967; **21**: 2695–2710.
48. Bürgi HB, Dunitz JD. Die strukturen der mittleren ringverbindungen. XVI. Cyclooctan-cis-1,2-dicabonsäure. *Helv. Chim. Acta* 1968; **51**: 1514–1526.
49. Egmond JV, Romers C. Conformations of non-aromatic ring compounds. LI. The crystal structure of trans-1,4-dichloro-cyclooctane at 180° *Tetrahedron* 1969; **25**: 2693–2699.
50. Wiberg KB. A scheme for strain energy minimization. Application to the cycloalkanes. *J. Am. Chem. Soc.* 1965; **87**: 1070–1078.
51. Bixon M, Lipson S. Potential functions and conformations in cycloalkanes. *Tetrahedron* 1967; **23**: 769–784.
52. Miller RW, McPhail AT. Crystal structure analyses and conformational studies of cis- cyclooctane-1,5-diol and cyclooctane-1,5-dione. *J. Chem. Soc. Perkin Trans.* **2**: 1979; 1527–1531.

